

This section discusses the spectral imager radiances and cloud products included in the **SSF** data set version Terra **Edition1A**. Additional information is in the [Description/Abstract Guide](#). The cloud parameters in the SSF are the result of convolving the values for the clear-sky and cloudy data derived for each 1-km MODIS pixel sampled every other pixel and scan line ([see Convolution Process](#)) to give an effective resolution of 2 km that matches that of VIRS. Five radiances taken at 0.65 (visible, VIS), 1.64 (near infrared, NIR), 3.75 (solar infrared, SIR), 11.0 (infrared, IR), and 12.0 (split-window channel, SWC)  $\mu\text{m}$ , channels 1, 6, 20, 31, and 32, respectively, are used for each MODIS pixel.

## Cloud Mask

Based on the values of these radiances, each MODIS pixel is classified as clear, cloudy, bad data, or no retrieval. Each clear pixel is categorized as weak, strong, snow, aerosol, smoke, fire, glint, or shadow. Cloudy pixels are categorized as weak, strong, or glint, where glint means that pixel was detected at an angle favorable for the viewing of specular reflection. Weak or strong categorizations indicate the degree of confidence in the selection. Atmospheric profiles of temperature, ozone, and humidity, model estimates of surface skin temperature, elevation, and one of the nineteen surface types ([CERES Surface Properties Home Page](#)) are also associated with each MODIS pixel. Trepte et al. (1999) discuss the general cloud-mask that is applied to VIRS and MODIS data in non-polar latitudes. The cloud masks used in polar regions are described in more detail by Trepte et al. (2001, 2002).

The cloud masks rely on comparisons of the observed radiances to estimates of the radiances for a cloud-free scene at a given pixel location and viewing and illumination conditions. These estimates are based on empirically derived maps of clear-sky overhead-sun spectral albedo, models of the solar-zenith angle (SZA) dependence of albedo (Sun-Mack et al. 1999; Chen et al. 2002a), and surface emissivities (Chen et al. 2001, 2002b) that use the MOA input. A few improvements in the clear-sky reflectance predictions and the mask algorithms have been developed for MODIS Edition1A processing. The clear-sky ocean reflectance model used for VIRS Edition2 was reduced in magnitude by 13% to account for the spectral differences between the VIRS and MODIS VIS channels (Chen et al. 2002a). Clear-sky snow reflectances are predicted using a model that is tuned to the MODIS observations (e.g., Trepte et al. 2001; Spangenberg et al. 2001). The twilight cloud masks are now applied for SZA between  $82.0^\circ$  and  $88.5^\circ$  instead of the range of  $82.0^\circ$  -  $87.5^\circ$  used for VIRS Edition2.

Bad-data pixels are those having at least one radiance that was set to a default value or was outside of the allowed range. The greatest problem causing bad data was the saturation of the thermal channels over land. The saturation temperatures for the Terra MODIS channels 20, 31, and 32 are 321.4, 324.9, and 319.4 K, respectively. Because of its relatively low maximum temperature and its reflected solar component, the 3.7- $\mu\text{m}$  channel was often saturated during midday over deserts and scrubland. No-retrieval pixels are those that are initially identified as cloudy, but their radiances cannot be interpreted with the theoretical models used to derive cloud particle size and optical depth.

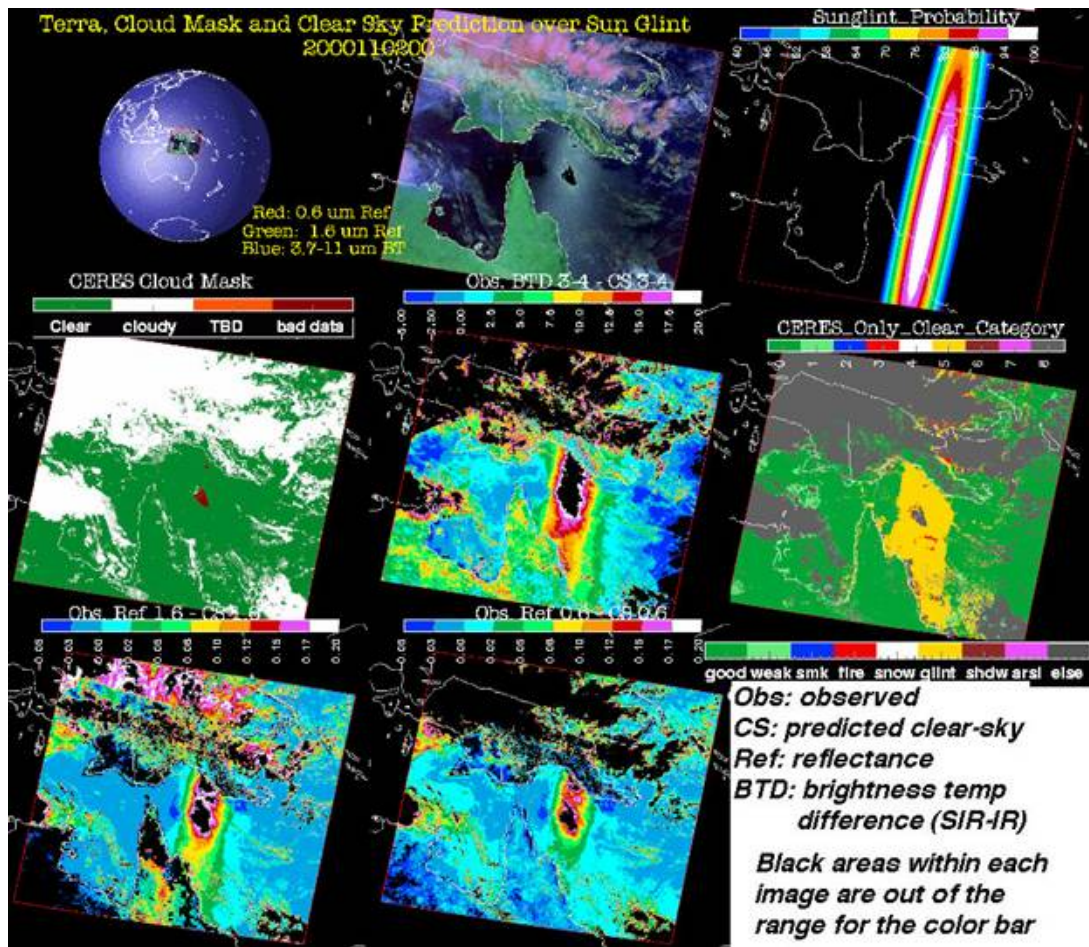


Fig. 1. CERES cloud mask and comparison of predicted clear-sky and observed radiances for Terra MODIS data taken around northern Australia, 0000 UTC, 2 November 2000.

An example of the results for the non-polar daytime cloud mask applied to an area off the coast of northeastern Australia is shown in Fig. 1 for Terra MODIS data taken around 0000 UTC, 2 November 2000. Differences between the predicted clear-sky and observed reflectances and brightness temperature differences (BTD) are also shown for comparison. The clear pixels are categorized as good or strong, weak, and fire (red areas) in this example. The fire pixels are actually pixels that are classified as sunglint in the latest mask improvement for MODIS. Over land areas, they would truly correspond to a fire classification. The area of sunglint probability in Fig. 1 is valid only for probabilities greater than 40% for a specific wind speed. The CERES mask actually tests for glint out to the 10% probability level. Hence, the clear glint classification area exceeds that encompassed by the 40% contour. The bad-data area coincides with the maximum sunglint probability. Except for cloudy and strong sunglint areas, the predicted clear-sky reflectances are generally close to the observed values. The SIR-IR BTDs in some land areas were overestimated, probably as a result of errors in the MOA-predicted surface skin temperatures.

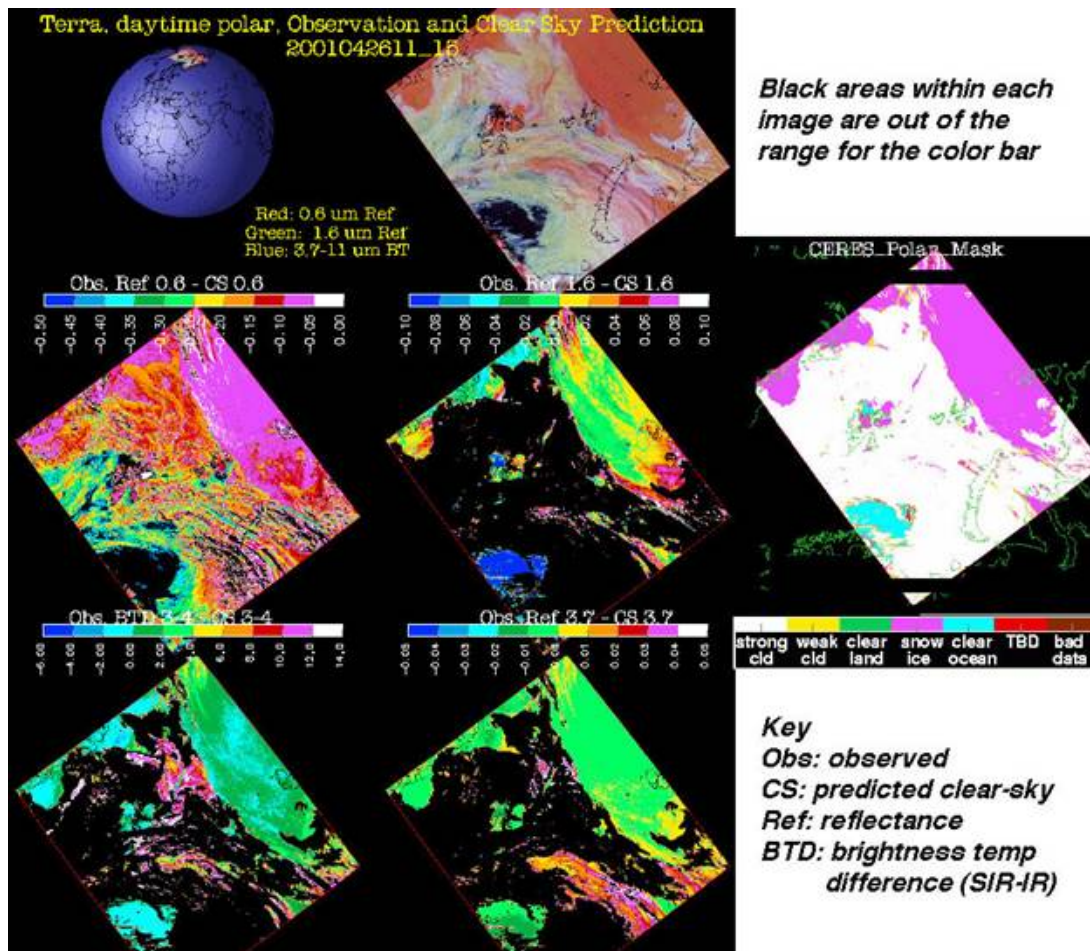


Fig. 2. CERES daytime polar mask and differences between predicted clear-sky and observed radiances for MODIS data over the Arctic Ocean, 1100 UTC, 26 April 2001.

Figure 2 shows the results for the daytime polar mask applied to MODIS data over the Arctic Ocean north of Russia at 1100 UTC, 26 April 2001. The differences between the predicted clear-sky radiances and temperature differences are also given. The clear-sky reflectance and brightness temperature differences (BTD) for the 3.7- $\mu\text{m}$  channel are very close to the observed values over clear areas. If the observed clear-sky VIS and NIR reflectances differ significantly from the predicted values, the overhead-sun albedo maps are updated to account for changes in the surface albedo relative to the *a priori* or previous value. The surface skin temperature is also computed for each clear pixel.

## Cloud Property Retrievals

The following values are computed for each cloudy pixel: phase (ice or water), VIS optical depth  $\tau$ , IR emissivity, liquid or ice water path  $WP$ , effective droplet radius  $r_e$  or effective ice crystal diameter  $D_e$ , cloud-top pressure, effective cloud height  $z_c$  and temperature  $T_c$ , and cloud-base and top pressures,  $p_b$  and  $p_t$ , respectively. Normally, the cloud phase, temperature, effective particle size and optical depth are computed using the VIS-IR-NIR-SWC Technique (VISST). The VIS channel is primarily used to estimate  $\tau$ ; the IR channel is for  $T_c$ , and the NIR channel is used for the particle size (Minnis et al. 1995), and the SWC is used to help the phase selection. Cloud height and pressure are found by matching  $T_c$  to an altitude in MOA vertical profile of temperature for the pixel location and time. The basic approach for deriving optical depth from the VIS reflectance for VIRS Edition2 and MODIS Edition1A follows the methodology outlined by Minnis et al. (1993a) but includes a more accurate surface-cloud-atmosphere reflectance parameterization (Arduini et al. 2002). Water and ice solutions are computed for each pixel and the phase is selected based on the solutions and several other criteria. Each pixel is initially analyzed with the layer bispectral threshold method (LBTM, see Minnis et al. 1993b) and assigned an initial cloud height classification that is used in later steps to aid the phase identification. The LBTM carries more weight in the MODIS Edition1A phase algorithm than in the VIRS Edition2 methodology. The cloud reflectance and emittance models of Minnis et al. (1998) were updated for the VIRS spectral channels to use in the VIRS Edition2 processing. The SIR reflectance models were updated for the MODIS spectral bandpass and cloud reflectance models were also developed for the MODIS and VIRS NIR filter functions. The VIRS cloud emittance models are used for the MODIS Edition1A processing. Corrections for atmospheric absorption use radiative transfer calculation employing the correlated  $k$ -distribution method (Kratz, 1995) with the absorption coefficients reported by Minnis et al. (2002a, b).

If the underlying surface is determined to be snow- or ice-covered either from the snow-ice maps or from identification of nearby pixels as clear snow, then the SIR-IR-NIR Technique (SINT) is applied. In this approach pioneered by Platnick (2001), the NIR channel replaces the VIS channel for optical depth determination. Use of the VISST over snow typically overestimates the cloud optical depth (e.g., Dong et al. 2001).

To illustrate the retrievals and some of the problems encountered, examples for midlatitude, tropical western Pacific (TWP), and Arctic areas are given in Figs. 3, 4, and 5, respectively. The midlatitude area includes the Atmospheric Radiation Measurement (ARM) Program Southern Great Plains Central Facility (SCF) in north central Oklahoma., while the Pacific area includes the ARM TWP site on Manus Island. The ARM North Slope of Alaska (NSA) site at Barrow, Alaska is in the Arctic region in Fig. 5. The ARM sites are being used for validation of the CERES cloud and radiation products.

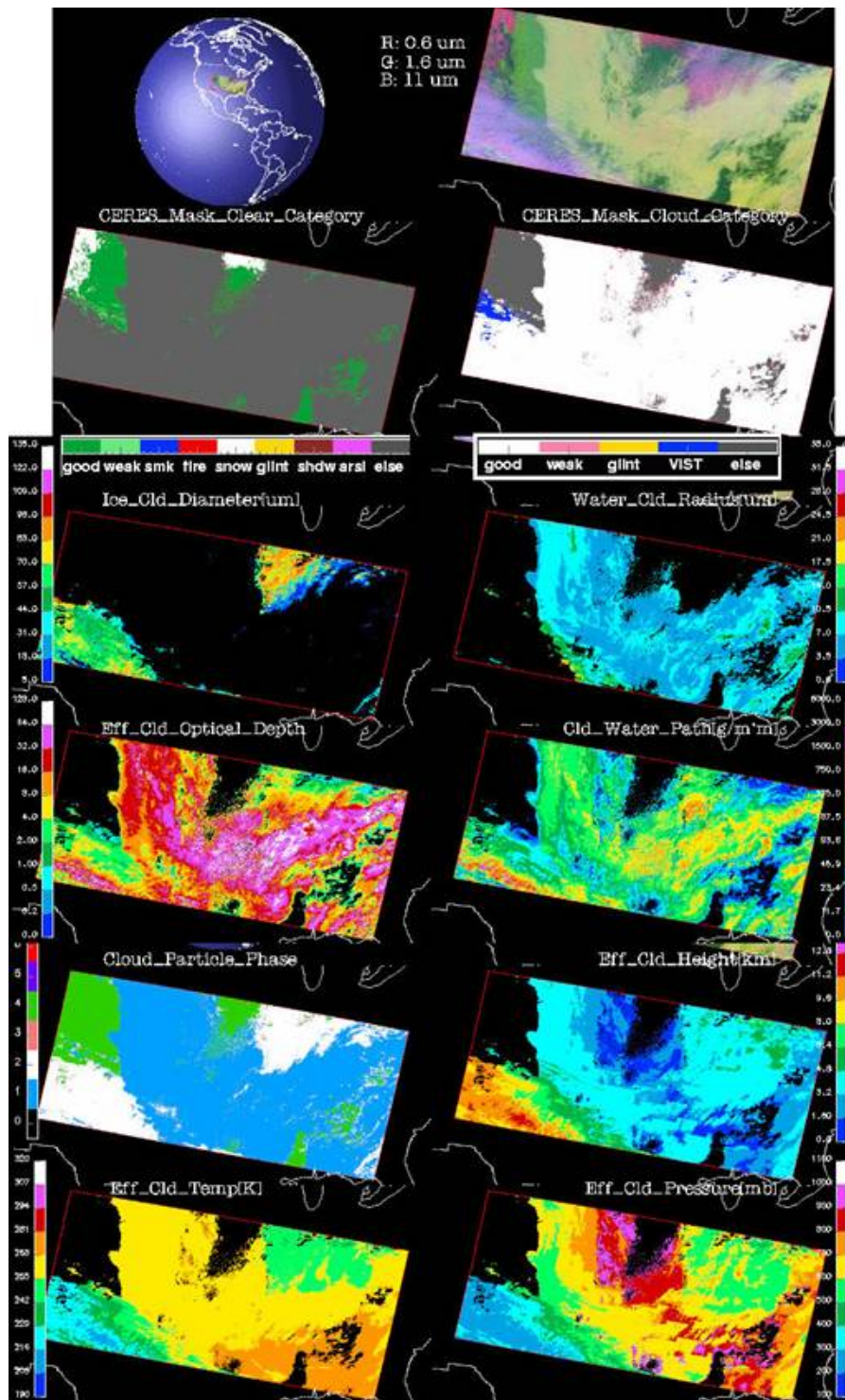


Fig. 3. Cloud properties over south central USA from MODIS, 1700 UTC, 2 December 2000.

The composite image in Fig. 3 shows areas of green, deep magenta, pink, and off white that generally correspond to clear land, snow, ice clouds, and low water clouds, respectively. This correspondence is reflected in the clear and cloudy category and phase pictures. Most of the clouds are classified as good. The pink areas seen around cloud edges and among scattered clouds indicate that the classification of the pixels as clouds was weak. The VIST category (blue) indicates that the VISST or SINT was unable to arrive at a solution for those pixels and returned a no-retrieval flag. The VISST or SINT can fail to retrieve a solution in a variety of situations that include thin clouds over shadowed areas, shadowed low clouds, ice clouds over poorly characterized backgrounds (e.g., retrieval assumes snow and the surface is snow free or vice versa, highly inaccurate skin temperature), and large SZA or viewing zenith angle (VZA) for a scene with significant vertical structure. This scene contains both single- and multilayered clouds, but the CERES algorithm determines the properties based on the assumption of a single-layer cloud. In areas where the cloud is truly only one layer or the upper layer is optically thick, the results are usually relatively consistent with expectations and should be fairly accurate. However, when the cloud system consists of ice-over-water clouds, the retrieval is a compromise between the water and ice solutions (e.g., Kawamoto et al. 2002). This compromise is evident in Fig. 3. The values of  $r_e$  generally vary between 5 and 10  $\mu\text{m}$  for the extensive low-level, mostly supercooled cloud deck ( $255\text{ K} < T_c < 268\text{ K}$ ). The cirrus clouds in the lower-left quadrant and the upper-right quadrant overlap some portions of the low-level clouds. In most of the overlap cases on the left, the phase selection is for liquid water and  $r_e$  varies from 10 up to 25  $\mu\text{m}$ . For the overlapped pixels classified as ice,  $D_e$  is around 35  $\mu\text{m}$  compared to values exceeding 45  $\mu\text{m}$  for the presumably non-overlapped cirrus clouds in that sector. The derived values of  $T_c$  and  $z_c$  for the overlapped clouds fall between the 8-13 km non-overlapped cirrus and the 3.5-km stratus.

For the cirrus in the upper-right quadrant, some of the overlapped ice clouds are diagnosed with effective diameters as small as  $10\ \mu\text{m}$  compared to  $D_e > 90\ \mu\text{m}$  over some of the thicker portions of the cirrus clouds. The cirrus in this case are apparently not much higher than the stratus deck, at least in radiative terms. As will be shown later, the derived cloud height for the stratus deck may be overestimated due to the sounding used in the retrieval. The  $z_c$  and  $p_t$  fields are generally smooth except for some of the stratus cloud areas where the values vary in a blocky fashion. This type of structure generally arises from differences in the MOA soundings between adjacent  $1^\circ$  regions. Some of the soundings may properly capture boundary-layer inversion structures while others will not. The resolution and accuracy of the sounding is crucial for properly converting  $T_c$  to  $z_c$  when boundary-layer inversions are present (e.g., Garreaud et al. 2001).

A problem that arises for supercooled clouds involves the phase selection for pixels that include the edges of a cloud or a portion of a small cloud. The partially-cloud filled pixels will often cause an overestimate of  $r_e$  and, when the cloud is supercooled, the value may be so large that the phase selection is tipped to the ice classification. Thus, along the edges of some supercooled cloud decks, the clouds may be classified as ice clouds as seen in the phase picture in Fig. 3. One solution for this effect might be the use of the MODIS 250-m VIS pixels to estimate the fractional cloudiness within each 1-km pixel (e.g., Nguyen et al. 2002).

Over the TWP (Fig. 4), the water-droplet effective radii generally range between  $9$  and  $16\ \mu\text{m}$  with some larger values evident in overlapped cases. Some very small ice crystal diameters are also retrieved for other overlapped pixels. Values of  $WP$  exceed  $3000\ \text{gm}^{-2}$  in some areas with large cloud optical depths. The cloud water path is computed based on the retrieved particle size and optical depth (Minnis et al. 1998). Thus, if the cloud is identified as an ice cloud, then  $WP$  is computed assuming the entire column is filled with a cloud having the retrieved value of  $D_e$  and  $\tau$ . For overlapped clouds or convective clouds, the column will often consist of a thick layer of liquid water topped by an ice cloud. Since the ice cloud particles are usually larger than their liquid counterparts, the  $WP$  computed for the entire cloud can be overestimated with this approach. This overestimation is probably compensated to some extent in that, for a given radiance, the ice-cloud optical depth is often much smaller than the water-cloud optical depth. The full impact of the single-phase assumption on  $WP$  requires additional study.



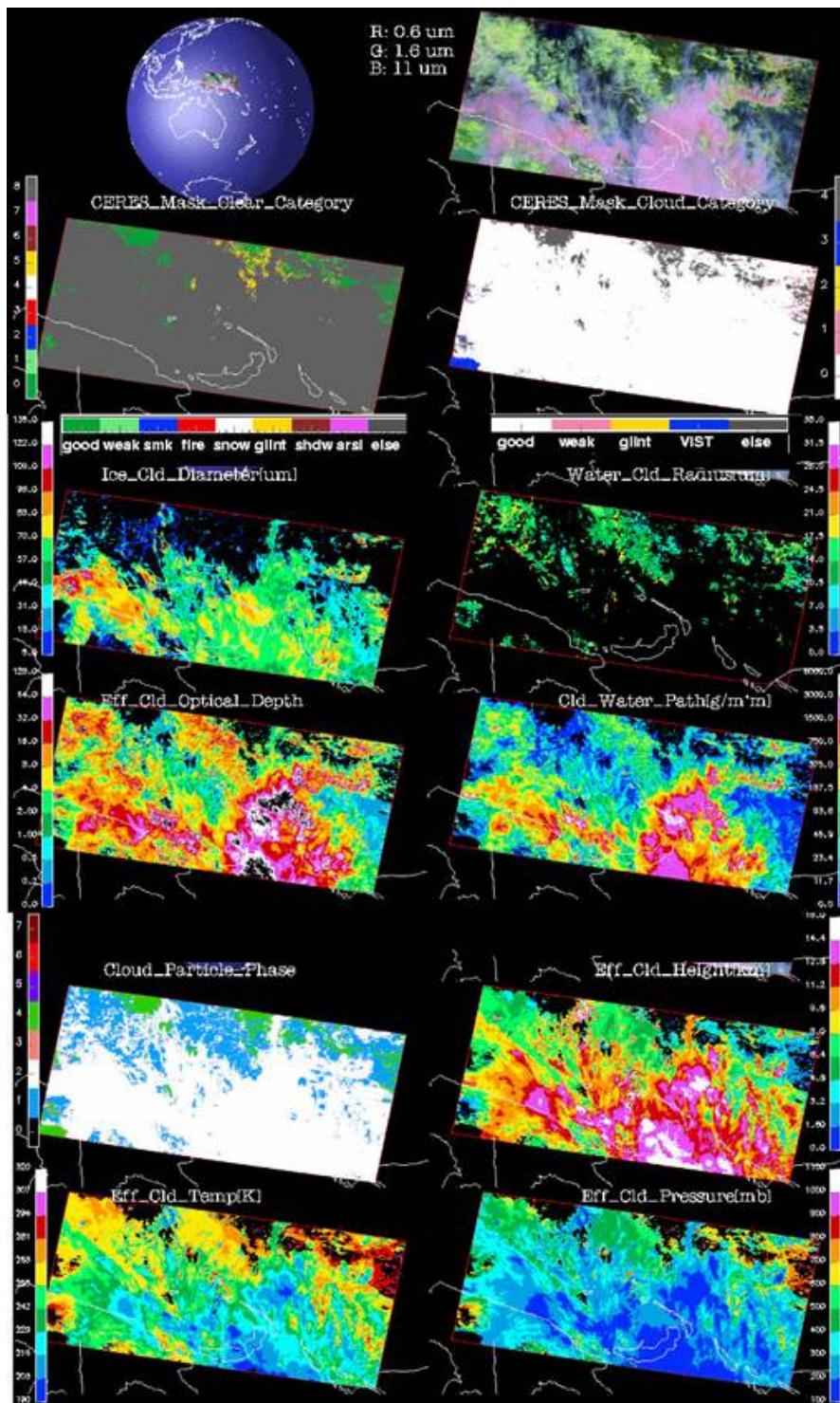


Fig. 4. Cloud properties over tropical western Pacific from MODIS, 0000 UTC, 6 December 2000.

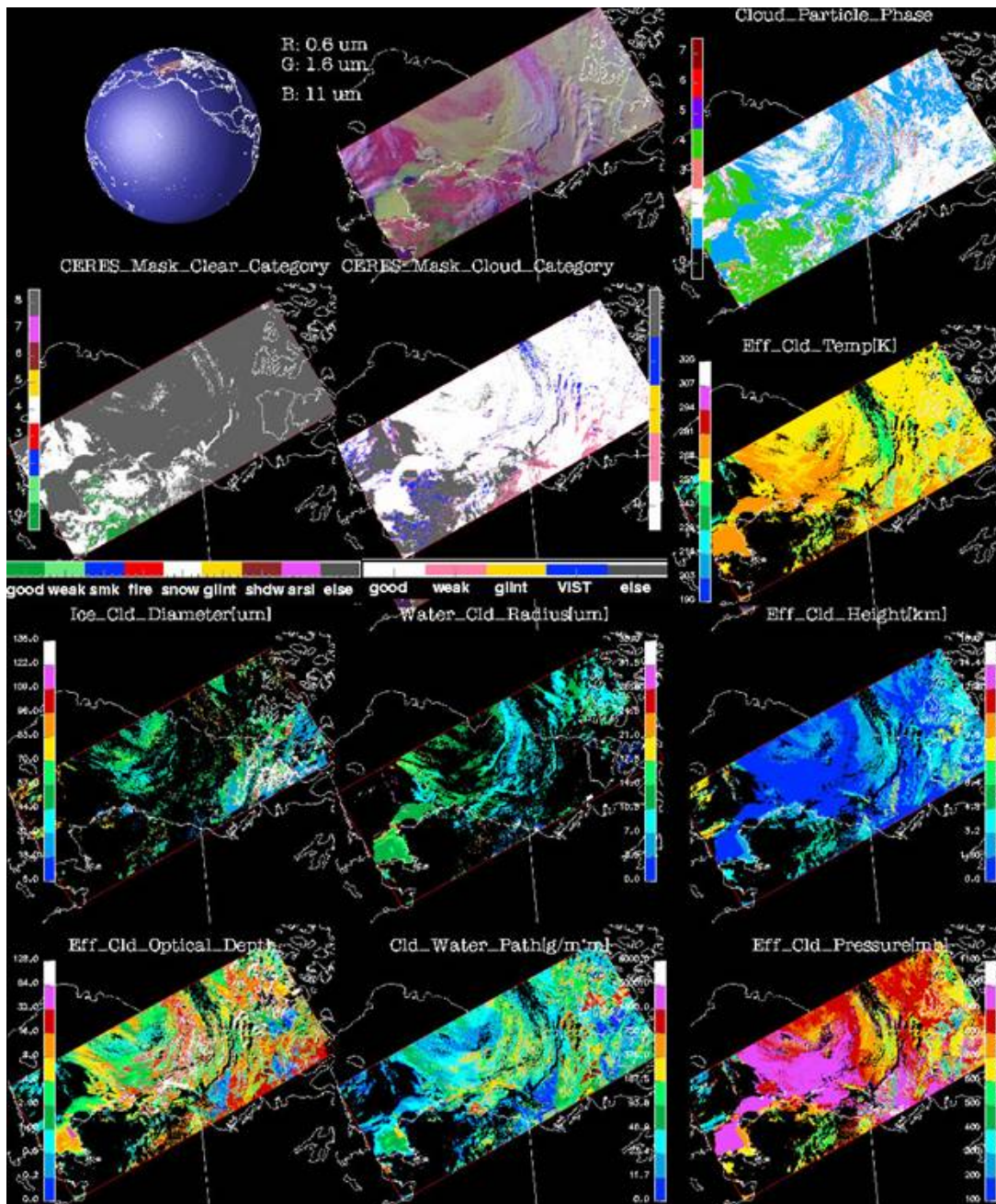


Fig. 5. Cloud properties over Alaska & Arctic Ocean from MODIS, 0600 UTC, 2 June 2001.

The retrieval difficulties encountered in the midlatitudes and Tropics are exacerbated in polar regions. As seen in Fig. 5, the background is more variable and cloud shadowing is more prevalent because the SZA's are higher, on average, than elsewhere. Phase selection and retrievals are more difficult for thin clouds over snow than for other surfaces. Inversions are more prevalent and the vertical profile of temperature is more isothermal. For these reasons, more no-retrievals and weak-cloud classifications occur over polar regions.

## MODIS Data

The cloud products rely on accurately calibrated imager radiances. Terra MODIS validated radiance data were used for Edition1A analyses. The MODIS thermal infrared channels are calibrated with onboard blackbodies and the solar channels are calibrated approximately once per month using a solar-viewing diffuser. Space looks provide zero radiance levels for the calibrations (Butler and Barnes, 1998). Wan et al. (2002) provide a preliminary calibration assessment of the MODIS thermal infrared channels for data taken during May and June 2000. The nominal MODIS calibrations were compared to other calibrated satellite data to determine stability and relative gains to detect any inconsistencies with other commonly used imagers. During the period from May 2000 through July 2001, the VIRS solar and infrared channels were compared to collocated and co-angled radiances from the eastern Geostationary Operational Environmental Satellite (GOES-8) and the Visible Infrared Scanner (VIRS) on the Tropical Rainfall Measuring Mission (TRMM) satellite. An initial analysis indicated that all of the MODIS channels are stable and very similar in response to the corresponding VIRS and GOES-8 channels, except for the VIRS 1.6- $\mu\text{m}$  channel, which appears to have a significant calibration bias. The GOES-8 was calibrated against the ATSR-2 on a monthly basis since 1995 to establish a trend line in the GOES gain. Thus, comparison of GOES and VIRS is equivalent to comparing ATSR-2 and VIRS over ocean for purposes of detecting long-term trends, because both VIRS and ATSR-2 use diffuser systems for calibrating their visible channels. Spectral differences were normalized for all of the imager comparisons. Except for the near-infrared gain changes, details of the calibration studies for

each channel including comparisons with the MODIS channels are given by Minnis et al. (2002a, b). The following remarks summarize the basic findings.

**Ch. 1, VIS (0.65  $\mu\text{m}$ ):** The MODIS visible (VIS) channel reflectance has been compared with the corresponding VIRS channel for December 2000 through March 2001 following the approach of Minnis et al. (2002a). No statistically significant trend was observed in the slope between the two sensors for that time period. The MODIS reflectance exceeds the VIRS reflectance over bright scenes and vice versa for darker scenes (Minnis et al. 2002a). Most of the VIRS excess reflection for dark scenes is due to strong Rayleigh scattering in the VIRS window relative to that for MODIS. The excess reflectance for MODIS relative to that for VIRS in brighter scenes appears to be a calibration difference. Therefore, the optical depths retrieved for thicker clouds should be somewhat larger from MODIS than from VIRS for the same scenes.

**Ch. 2, NIR (1.64  $\mu\text{m}$ ):** The comparisons of MODIS and ATSR-2 NIR reflectances with VIRS are very consistent indicating that both the MODIS and ATSR-2 NIR reflectances exceed their VIRS counterparts by 15-17% as of late 2000. Comparisons of VIRS and MODIS retrievals show that the VIRS reflectances are unrealistic and that the MODIS calibration yields cloud particle sizes that are consistent with those derived with other channels (Young et al. 2002). Further comparisons show that the VIRS 1.6- $\mu\text{m}$  calibration is degrading relative to MODIS. As of June 2002, the slope  $G$  of the regression line

$$LT = G L2' + I$$

is

$$G = 0.000135 D + 1.098,$$

where  $D$  is the number of days since January 1, 2000,  $LT$  is the Terra MODIS NIR radiance,  $L2'$  is the VIRS radiance (in  $\text{W m}^{-2} \text{sr}^{-1} \mu\text{m}^{-1}$ ) corrected for the VIRS thermal leak and differences in the spectral response function between MODIS and VIRS, and the offset,

$$I = 0.214 - 0.000354 D.$$

Until indicated otherwise, it is assumed that the MODIS NIR calibration is correct and stable.

**Ch 20, SIR (3.75  $\mu\text{m}$ ):** The SIR channel is very similar to, but narrower than the VIRS 3.7- $\mu\text{m}$  channel. Wan et al. (2002) suggest that the absolute value of the SIR radiances are biased high by 2 - 3%, equivalent to  $\sim 0.6$  K at 283 K. Minnis et al. (2002b) found that the MODIS channel 20 was 0.2 K colder than VIRS channel 3 at 300 K and 1.3 K warmer at 200 K during 2000. Such differences will introduce some discrepancies between the VIRS and MODIS retrieved cloud properties. Theoretically, the two sensors should measure brightness temperatures to within 0.1 K of each other for clear and cloudy atmospheres. Since January 2001, VIRS has been averaging almost 1.0 K colder than MODIS in the SIR temperatures both during daytime and at night. It is not clear if MODIS or VIRS has changed in calibration.

**Ch 31, IR (11.0  $\mu\text{m}$ ):** Wan et al. (2002) found that the MODIS infrared (IR) channel was accurate to  $\sim 0.4\%$  or to  $\sim \pm 0.2$  K. Minnis et al. (2002b) found that MODIS is roughly 0.4 K colder than VIRS at 300 K and differs by 0.0 K at 200 K. Theoretically, it appears that MODIS should be 1.0 K colder than VIRS at all temperatures. A later analysis shows no trends in the average difference between MODIS and VIRS IR temperatures through June 2002. At night, the difference is 0.0 K, while during the day, VIRS is 0.3 K warmer than MODIS.

**Ch 32, SWC (12.0  $\mu\text{m}$ ):** Wan et al. (2002) found that the MODIS split window channel (SWC) was also accurate to  $\sim 0.4\%$  or to  $\sim \pm 0.2$  K. MODIS is roughly 0.8 K and 0.7 K warmer than VIRS at 300 K and 200 K, respectively (Minnis et al. 2002b). Theoretically, it appears that MODIS should be nearly the same at 200 K and 0.5 K warmer at 300 K. No significant trend is apparent in the differences. At night, MODIS is 0.6 K warmer than VIRS. It is 0.8 K warmer during the daytime.

## DATA PROBLEMS

MODIS data were not taken between June 16 and July 1, 2001.

## Cloud Parameters

Preliminary assessment of the uncertainties in some of the cloud parameters has been completed. Many other datasets must be compared with the CERES MODIS cloud analyses before final error numbers are assigned. The cloud parameters have been evaluated visually by comparing a large number of high-resolution images with pictures of derived cloud products over a selected number of regions to ensure that the results appear to be qualitatively consistent with the imagery (e.g., Figs. 1 -5). Some of the parameters have been compared with climatological values to obtain a rough quantitative evaluation. The results have also been averaged for various surface types and angular ranges to determine any systematic variability. The most quantitative evaluations use estimates of similar quantities derived from passive and active radiometric measurements at surface sites, in particular, the ARM Southern Great Plains (SGP) facility in central Oklahoma. The available results have been compared with the VIRS Edition2 quantities and are being documented in a paper currently in preparation. They are also compared here with MODIS Edition1A datasets. The results are similar to those found applying the CERES algorithm to GOES-8 data.

**Cloud amount** - Figure 6 shows compares the mean zonal cloud amounts from MODIS for June 1-16, 2001 with long-term averages of cloud amounts from surface observations (Hahn et al., 1999) and ISCCP D2 data (Rossow and Schiffer, 1999). The CERES amounts fall between the ISCCP and surface means between 20°S and 60°S and are slightly less than both datasets between 20°S and 60°S. The surface and CERES data are in relatively good agreement north of 60°N, but disagree during the austral night over Antarctica. Part of the differences are due to sampling. The Terra orbit was designed to maximize clear-sky observations over land, where minimum cloudiness often occurs during

mid-morning. Thus, the MODIS mean cloud cover should be smaller where land areas most common. The climatological averages of cloudiness over the Arctic during June are generally higher than can be determined using the ISCCP algorithm (e.g., Minnis et al. 2001), so the good agreement between CERES and the surface data north of 60°N compared to the ISCCP results is not surprising. Both ISCCP and CERES retrieve more cloud cover during the austral night than is seen climatologically. However, the surface sampling over Antarctica and south of 30°S is very sparse, so the climatological values there may not be accurate representations of the zonal means.

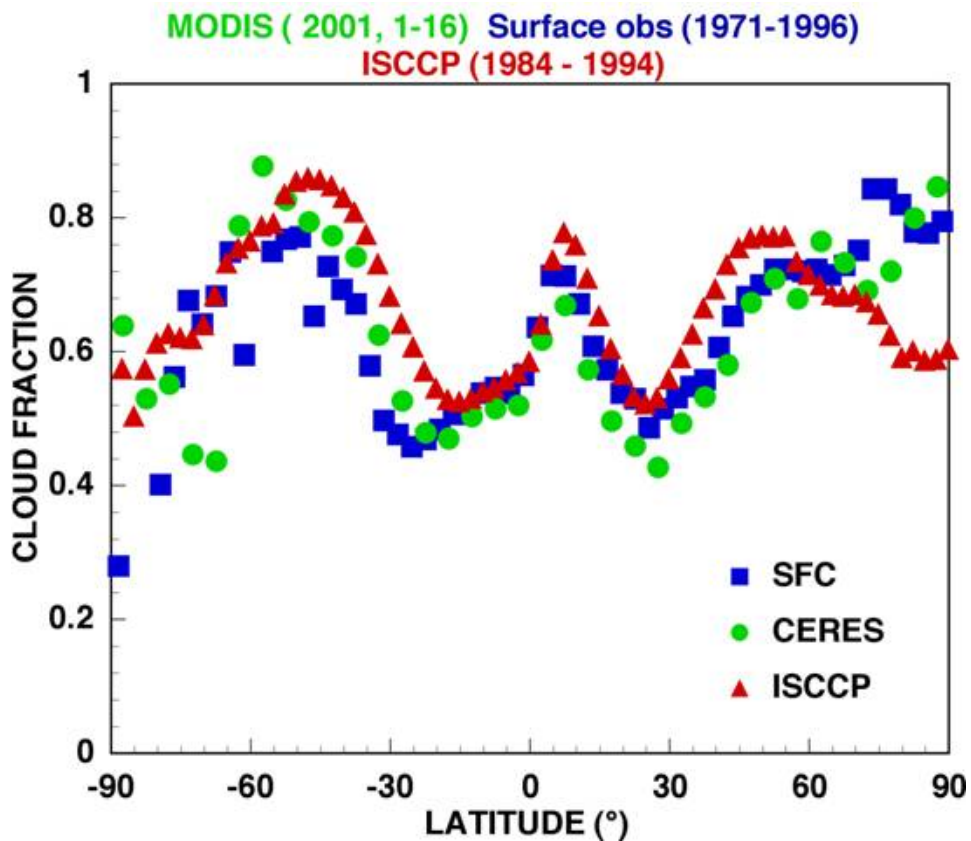


Fig. 6. Mean June cloud fractions from surface observations, ISCCP, and CERES MODIS.

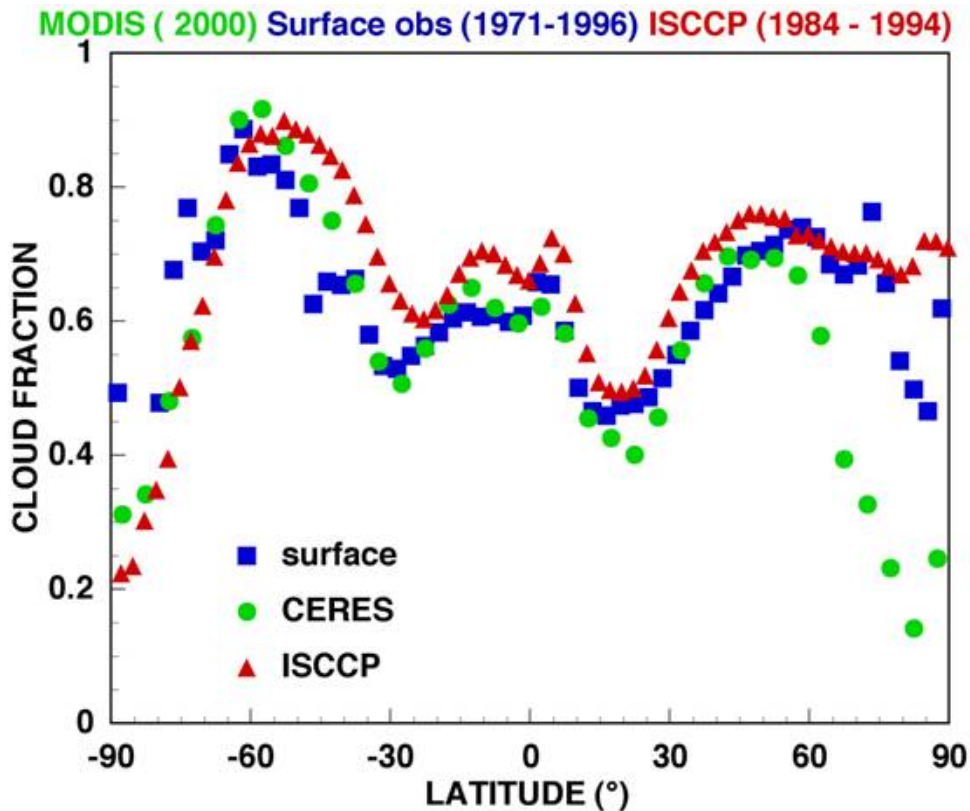


Fig. 7. Mean December cloud fractions from surface observations, ISCCP, and CERES MODIS.

The comparisons for the December 2000 retrievals (Fig. 7) produce similar results except that there is closer agreement between the surface

and CERES means between 60°S and 60°N. Both CERES and ISCCP tend to underestimate the cloudiness over Antarctica south of 80°S, but only the south pole is sampled by the surface. CERES grossly underestimates the cloud cover during the boreal night compared to both the surface and ISCCP means. This indicates a problem with the CERES nighttime polar mask. Users should be aware that the cloud amounts are underestimated north of 60°N when SZA > 82°. This effect may be present over Antarctica to some extent but does not appear to be as large as it is over the Arctic (Fig. 6). Examination of the data indicates that very low clouds and thin high clouds are most often missed over the Arctic at night. This error in cloud amount should have minimal impact on top-of-atmosphere flux calculations but may affect the computation of downwelling longwave flux at the surface. The thresholds will be altered to effect a better estimate nighttime polar cloudiness in the next CERES MODIS edition. The comparisons in Figs. 6 and 7 are summarized in Table 1, which shows that except for the Arctic night, the CERES mask produces cloud fractions that are much closer than their ISCCP counterparts to the surface observers' climatological estimates. This result is very much like that found for the VIRS Edition2 results. The ISCCP averages are most likely higher than the CERES values because ISCCP uses a larger pixel size (4- 10 km) and views many areas at high VZAs.

**Table 1. Mean cloud amounts (%) for surface and satellite datasets.**

Domain	Surface (1971-96)	CERES MODIS 12/2000, 6/2001	ISCCP D2 (1984-98)
60°S - 60°N, December	60.6	62.5	66.9
90°S - 90°N, December	63.2	56.3	69.6
60°S - 60°N, June	60.5	60.7	67.9
90°S - 90°N, June	63.1	63.9	66.7

**Cloud phase** - This parameter is more difficult to evaluate because it requires either in situ or combinations of passive and active remote sensing data. Inspection of the results with coincident imagery indicates that, during the daytime, the cirrus clouds, even very thin ones, are generally identified as ice clouds. The edges of these clouds are occasionally classified as water clouds and the very thin cirrus over low clouds are sometimes classified as water clouds. The edges of supercooled water clouds are occasionally mistaken as ice clouds as noted earlier. At night, the phase classification is less reliable except when  $T_c < 233K$  (ice) or  $> 273K$  (liquid). The mean zonal daytime ice-cloud amounts from MODIS relative are compared in Fig. 8 with long-term (1971-1996) mean fraction of combined cirrus and cumulonimbus clouds from surface observations (Hahn et al. 1999). The surface and CERES cloud fractions are relatively close between 40°S and 30°N during December and June. The CERES ice cloud amounts are less than the surface means around 25°N probably as a result of sparse sampling of desert areas from the surface observations. CERES retrieves more ice cloud cover than surface high cloudiness south of 40°S. The differences north of 40°N switch signs from December to June. Although the available datasets do not provide for an ideal comparison, the results in Fig. 8 indicate that the retrieved phase is reasonable at least for most latitudes. More objective measures are needed for validating the cloud phase.

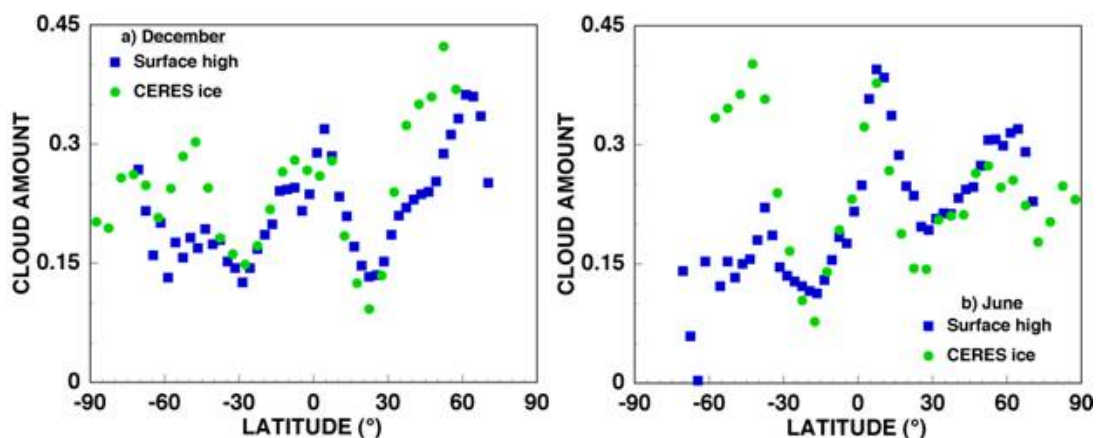


Fig. 8. Mean high (surface 1971-96) and CERES MODIS (12/2000, 6/2001) ice cloud amounts.

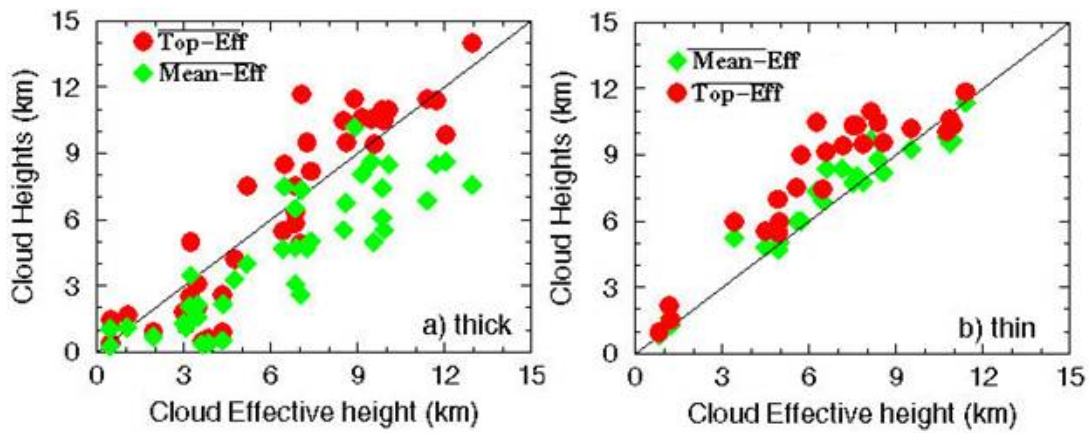


Fig. 9. Comparison of  $z_c$  and cloud heights from radar data over ARM SGP for a)  $\tau > 5$  and b)  $\tau < 5$ .

**Cloud height, pressure, temperature** - These parameters are all related because the cloud temperature is used to ascertain cloud height and the height is used to select the pressure. Effective cloud height derived from MODIS should be an altitude somewhere between the top and base of the cloud. It corresponds to the mean radiating temperature of the cloud. For water clouds, the mean radiating temperature is usually within a few 100 m of the top. For cirrus clouds, it can be close to the cloud base or near cloud top depending on the density of the cloud. Comparisons with the radar observations over the ARM southern Great Plains (SGP) site are shown in Fig. 9 for clouds observed during daytime. For the optically thick clouds ( $\tau > 5$ ),  $z_c$  is typically between the mean height and the top of the cloud except for some of the low cloud. For optically thin clouds ( $\tau < 5$ ),  $z_c$  is close to or slightly lower than the center of the cloud (Fig. 9b). At night,  $z_c$  is usually closer to the cloud top than the cloud center for thin clouds (not shown). For thick clouds at night (Fig. 10b), the top of the cloud and  $z_c$  are nearly identical except for some of the low clouds. The heights of several low clouds are overestimated by  $z_c$  during day and night. However, the temperatures for these same clouds (Fig. 10a) are typically equal to or greater than  $T_c$ . When  $T_c$  is nearly identical to the cloud center (mean) or top temperature, the surface and satellite heights should be the same unless the sounding used by the satellite retrieval misses the structure of the boundary-layer inversion, which is the case for several of the points in Fig. 10. If  $T_c$  is significantly colder than the mean and top temperature, then the surface-based radar may not be detecting a second cloud layer at a higher altitude. The errors in low-cloud heights due to inversions over oceans have been minimized with the use of a lapse rate technique (Minnis et al. 1992; Garreaud et al. 2001). A similar approach may be incorporated in the next MODIS Edition to reduce the errors in low cloud heights over land. Except for the low-cloud cases already discussed, nearly all of values of  $z_c$  were somewhere between cloud top and cloud base for the ARM SGP comparisons. The cloud temperature and height comparisons over the SGP are summarized in Table 1. Uncertainties in cloud-top pressure can be determined from the altitude differences in Table 1.

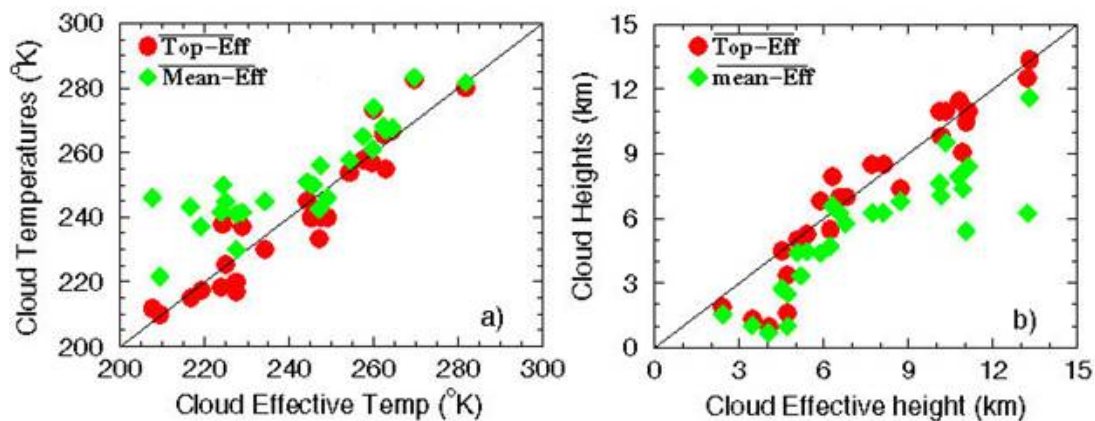


Fig. 10. Cloud temperature and height comparisons from radar data over ARM SGP for a)  $z_c$  and b)  $T_c$ .

Globally, at night, the mean effective cloud heights for liquid water and ice clouds are 0.6 km higher than their daytime counterparts. This difference is probably due to real diurnal changes in the vertical structure of clouds, but it also includes the differences in the thin-cloud height retrieval comparisons between day and night seen in Table 1. The nighttime method relies entirely on thermal channels, while the daytime algorithm uses both visible and thermal channels. The impact of a low cloud underneath a high cloud on the derived height is much greater during daylight because the low cloud adds to the optical depth, the parameter used to determine emissivity. At night, the surface and low-cloud temperatures are similar so that the optical depth, which relies on the cloud-top and surface temperature difference, is less sensitive to multilayered clouds. Thus, in areas where thin cirrus is prevalent over scattered low clouds or deserts where the surface emissivity is uncertain, the mean effective cloud heights are considerably greater than their daytime counterparts. Users should be aware of this day-night difference in cloud height. Previous methods, like that for the ISCCP, have used a single channel infrared temperature to assign cloud heights

at night resulting gross underestimates for optically thin clouds. The CERES approach represents an improvement over the single-channel technique.

**Cloud optical depth, effective particle size** - These parameters were also evaluated following the approach used by Dong et al. (2002) for comparing stratus cloud properties derived from GOES data with the CERES algorithm with retrievals of the same quantities from surface-based instruments at the ARM site using the techniques of Dong et al. (1997). Only single-layered stratus cloud comparisons were available at the time of this release. The stratus comparisons are summarized in Table 1. Overall, the agreement between the two datasets for stratus clouds is excellent during the daytime. Because the nighttime microphysical properties are limited, the comparisons are not reported here. The optical depths derived from MODIS are restricted to roughly 10 or less at night because of the limitations of infrared retrievals. Thus, estimates of  $r_e$ ,  $\tau$  and  $LWP$  from MODIS at night should not be used except for optically thin clouds. Generally, the standard deviations during the daytime are within the CERES accuracy goals. The MODIS and surface daytime retrievals agree at roughly same level as a similar comparison of surface, aircraft, and GOES retrievals for stratus over the same site (Dong et al. 2002). The number of samples here is still too small for this one site. These results represent only one set of climatological conditions. Dong et al. (2001) compared the retrievals of cloud droplet size and optical depth derived using the SINT over the Arctic ice pack and found good agreement with the surface and in situ data taken in the same area. Comparisons at the SGP and other sites are ongoing (e.g., Spangenberg et al. 2002) and will continue.

**Table 1: Uncertainties in cloud parameters based on comparisons at the ARM SGP site.**

	Mean difference (CERES- ARM)	Standard deviation	Standard deviation of difference (%)	N
<b>Day</b>				
Thin cloud temperature vs mean	7.0 K	6.4 K	-	27
Thick cloud temperature vs mean	-8.6 K	10.8 K	-	41
Thin cloud height vs. mean	-0.4 km	0.8 km	-	27
Thin cloud height vs. top	-1.6 km	1.3 km	-	27
Thick cloud height vs. mean	2.0 km	1.7 km	-	41
Thick cloud height vs. top	0.0 km	1.8 km	-	41
Stratus optical depth	-0.2	7.7	26	14
Stratus effective radius	-1.7 $\mu\text{m}$	2.8 $\mu\text{m}$	30	14
Liquid water path	-13 $\text{gm}^{-2}$	85 $\text{gm}^{-2}$	52	14
<b>NIGHT</b>				
Thin cloud temperature vs mean	-3.6 K	10.4 K	-	38
Thick cloud temperature vs top	1.1 K	7.3 K	-	28
Thin cloud height vs. mean	1.1 km	1.5 km	-	38
Thin cloud height vs. top	-0.2 km	1.5 km	-	38
Thick cloud height vs. mean	2.2 km	1.6 km	-	28
Thick cloud height vs. top	2.0 km	1.9 km	-	28

The surface-based cirrus retrieval method is limited to optically thin clouds and loses reliability for clouds with  $\tau > 3$ . The cirrus comparisons must be performed with extreme caution because of the variability of cirrus and because of the effect of clouds underneath the cirrus. The cirrus comparisons are underway and will be reported when available. Prior to CERES, the method for retrieving cirrus particle size, optical depth, and, hence, ice water path has been validated to some extent by comparisons with in situ and surface active remote sensors (Mace et al. 1998, Young et al. 1998). Duda et al. (2002) compared retrievals from MODIS with in situ data taken over Scotland and found excellent agreement between the in situ particle sizes and  $D_e$  for one case. Indirectly, it can be construed that the cirrus cloud optical depths are valid because the height corrections for the optically thin clouds place the clouds near the cloud center or between the cloud center and top. If  $\tau$  were overestimated, then  $z_c$  for the thin cirrus clouds in Fig. 9 and Table 1 would have been well below cloud center and, more often, below cloud base (e.g., Minnis et al. 1993). Thus, it is concluded that the cirrus cloud optical depths are reasonable. However, a more quantitative evaluation is underway using the SGP radar data and additional in situ data taken during recent field programs.

Minnis et al. (2002c) compared mean cloud optical depths from ISCCP and CERES. On average, the MODIS-derived values of  $\tau$  are 2 - 3 times greater than those from the ISCCP. The differences are probably due to calibration differences and to the cloud amount differences (Figs. 6, 7). For the same radiance, the optical depth would be smaller for greater cloud amounts.

## Angular Dependencies

MODIS on Terra provides the first opportunity to evaluate the angular dependencies of cloud properties from the CERES algorithms for VZAs out 65°. The VIRS was limited to VZA < 48°. Many of the same variations observed for VIRS (see [VIRS Edition2 data Quality Summary](#)) also occur for MODIS except that cloud amounts continue increasing from VZA= 48° to 65°. Values of  $r_e$  tend to increase slightly with VZA over ocean and decrease slightly over land, while  $D_e$  tends to increase with VZA over all surfaces (Fig. 11). The increase may be due to reduced effects of underlying water clouds on the ice particle size retrieval because of the increased path length. However, the ice cloud optical depths tend to decrease with VZA more so than for the water cloud optical depths. The net effect should be minimal variation of LWP or IWP with VZA. The variations of cloud properties with SZA are affected by the change of SZA with location. The angular variations for VZA, SZA, and relative azimuth angle are summarized by Heck et al. (2002). The VIRS dependencies discussed in the VIRS Edition2 DQS should be most valid for the SZA and relative azimuth angle variations.

Overall, the angle dependencies show that the derived cloud properties are reasonable at a level of 25% or better. More likely, the values are consistent at a higher level of accuracy because of the natural variability that occurs in clouds but is reflected in the angular dependencies (i.e., the SZA-diurnal variation, the RAZ-location variation). The VZA dependencies in cloud optical depth and cloud particle size are probably mostly due to the increase in cloud fraction with VZA. More optically thin or broken clouds are detected at higher VZAs resulting in a decrease of the mean  $\tau$ , which in turn would cause an apparent increase in the effective particle size. The ice crystal phase functions for CERES yield results that appear to be as representative as the water cloud phase functions because the variations of  $D_e$  with any particular angle are no worse than the variations in  $r_e$ . This result is consistent with the findings of Chepfer et al. (2002).

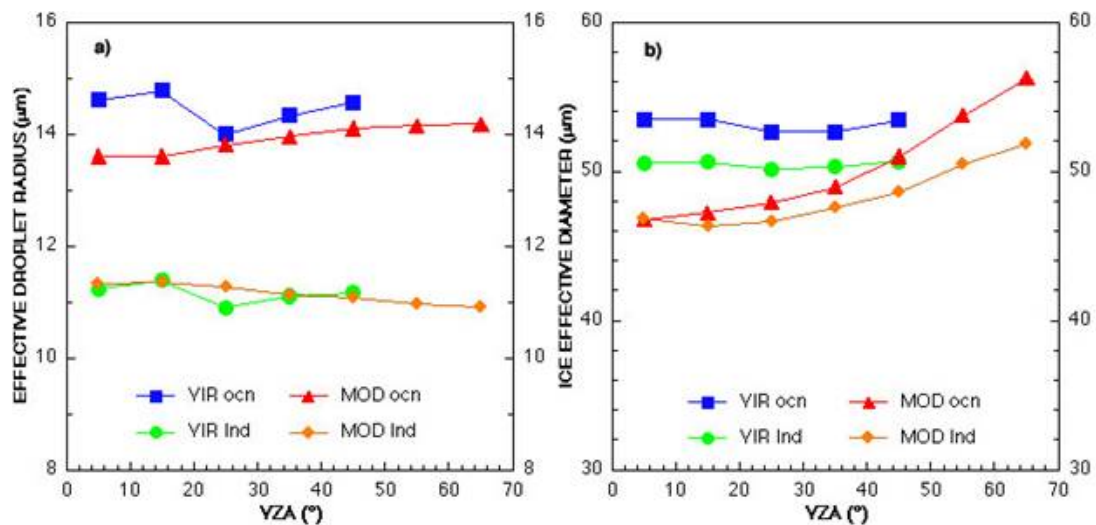


Fig. 11. VZA dependence of mean cloud properties from MODIS & VIRS, December 2000.

## Consistency with VIRS

One of the goals of the CERES program is to provide a continuous series of cloud and radiation measurements that are consistent from one satellite to another. The VIRS Edition2 zonal mean results for December 2000 and June 2001 have been compared to those from MODIS Edition1A products for the same time period to provide a measure of the consistency in the results for the two instruments. Figures 12-17 show the comparisons for June 2001. The MODIS values are based on the first 15 days of the month. The mean total cloud amounts track each other very closely in the southern hemisphere except at 37.5° S where VIRS data only cover the northern half of the zone. The larger cloud amount from MODIS is reasonable given the zonal gradient. Greater differences are evident in the northern hemisphere, especially if land and ocean are separated (bottom panel). The MODIS cloud amounts are smaller over both land and ocean. A large portion of the differences is most likely due to the differences in sampling since MODIS only samples near 1030 LT, while the VIRS samples different parts of the zones at different times of day. Presumably, MODIS measures the minimum cloud amount during the day, especially where deep convection is prevalent. The zones of disagreement change with the season (not shown).

The mean cloud heights (Fig. 13) are generally in good agreement with the small differences over ocean for liquid water clouds. MODIS measures slightly greater ice cloud heights over the ocean, but slightly lower heights over land. Convection over land would tend to yield lower water cloud heights at 1030 LT compared to an average over the entire day (VIRS). The MODIS water cloud optical depths (Fig. 14) are very close to those from VIRS over the ocean and land except in the extreme portions of the southern hemisphere. The ice clouds over ocean have nearly identical optical depths, on average, from the two instruments. Over land, MODIS yields slightly smaller optical depths on average. In the northern hemisphere, the MODIS ice clouds are not as thick as those measured by VIRS while the reverse is true south of 25°S. Again, the sampling patterns are consistent with the differences. Figure 15 shows the zonal mean particle sizes for the two instruments. The MODIS-derived water droplets over land and ocean are approximately 0.6-µm smaller than their VIRS counterparts. Over ocean, VIRS yields slightly smaller ice crystals on average. The ice crystals from MODIS are significantly smaller over land compared to those from VIRS. If deep convection is responsible for generating larger crystals, then the absence of such convection at 1030 LT might explain some of the difference over land. Another explanation may be that overlapped clouds over land tend to contain more ice during the late afternoon when convection is most active and, therefore, the derived ice crystal size, on average, is less affected by the presence of an underlying water-droplet cloud. Such diurnal effects need closer examination.

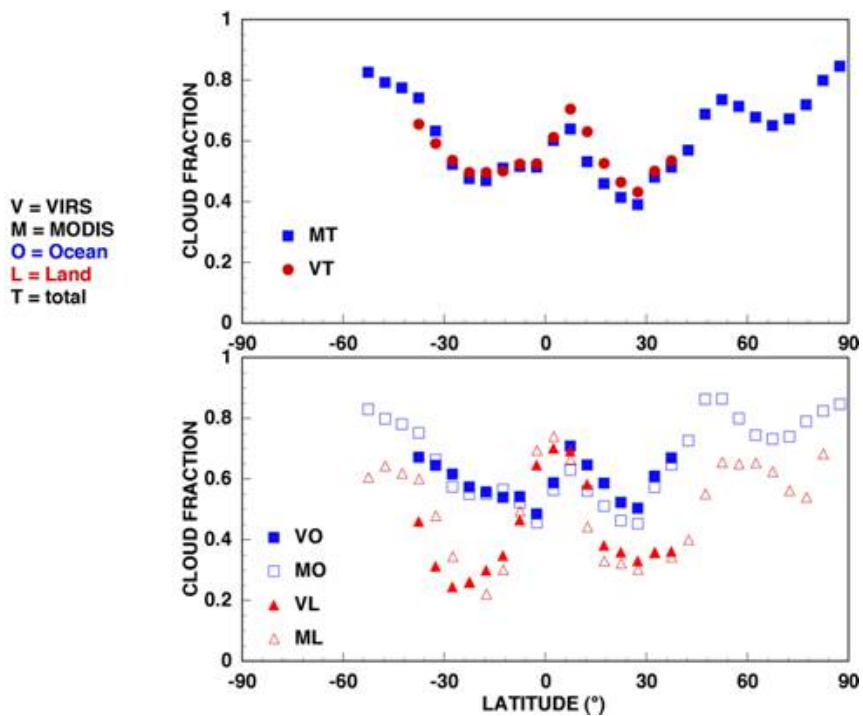


Fig. 12. Zonal mean daytime cloud amounts from MODIS and VIRS, June 2001.

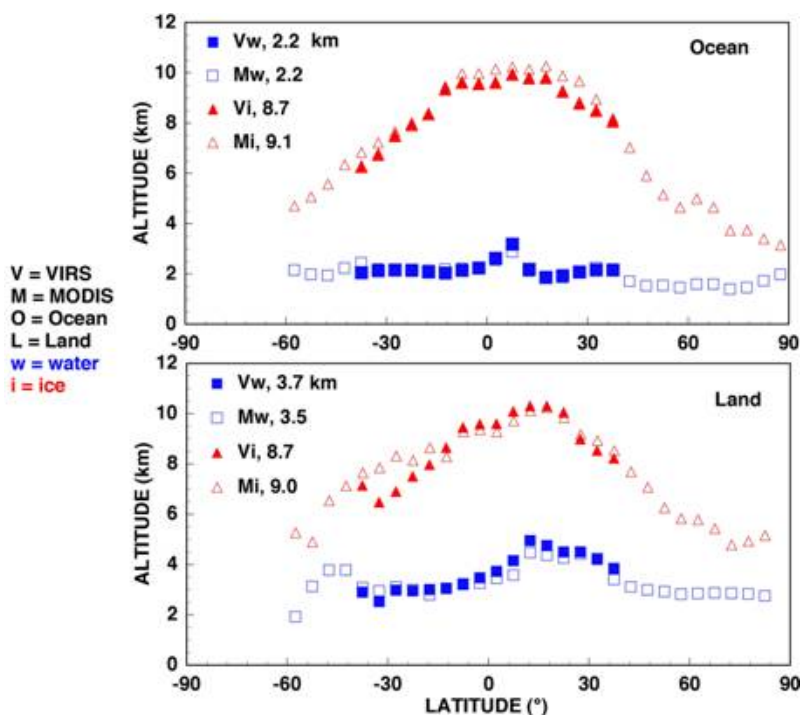


Fig. 13. Zonal mean daytime cloud effective heights from MODIS and VIRS, June 2001.

The derived water path results in Fig. 16 show generally good agreement except for south of 25°S where MODIS appears to produce much greater values of both liquid WP (LWP) and ice WP (IWP). These differences are most likely due to poor sampling by VIRS in the southern hemisphere. The mean differences are very reasonable outside of the 25°S - 37.5°S zone. The sampling from VIRS needs closer scrutiny. The IWP differences are consistent with the  $D_e$  and  $\tau$  differences. The mean cloud fractions are plotted according to phase in Fig. 17. Again, the differences are small except in the far south, where MODIS detects far more ice clouds resulting in a skewed average overall. Other differences are consistent with the diurnal considerations.

To minimize the sampling effects, the VIRS and MODIS results were compared directly where the Terra and TRMM paths crossed within an hour of each other. The values for each parameter were averaged over 0.25° regions to reduce the effects of the time differences. Figure 18 shows the scatterplots of the ice and water cloud optical depths and particle sizes for two scenes that had viewing time differentials of 31 (upper panel) and 45 (lower panel) minutes. The scatter in the results arises from changes in the scene between the overpass times and

differences in the viewing conditions between the two instruments. Results from a closer match (3 minute differential) are plotted in Fig. 19. The VIRS water droplets tend to be nearly 0.5- $\mu\text{m}$  larger than their MODIS counterparts in Fig. 18, a result consistent with the zonal mean differences. The VIRS droplets are 1.4- $\mu\text{m}$  larger in Fig. 19 when the two instruments have a better time match. The difference in this case may be due to the 90° differences in the viewing geometry. The optical depth differences are extremely small for both ice and water clouds in Fig. 19, but the mean ice crystal size is much smaller from VIRS. The small amount of sampling in this instance precludes conclusions about the differences. The greater number of samples in Fig. 18 is accompanied by more scatter in the results. The mean values of  $D_e$  are within 1  $\mu\text{m}$  of each other while the optical depth differences vary considerably with MODIS larger, on average. Nevertheless, the results are generally very consistent and within the tolerances needed to produce a cloud-radiation dataset that is consistent across platforms.

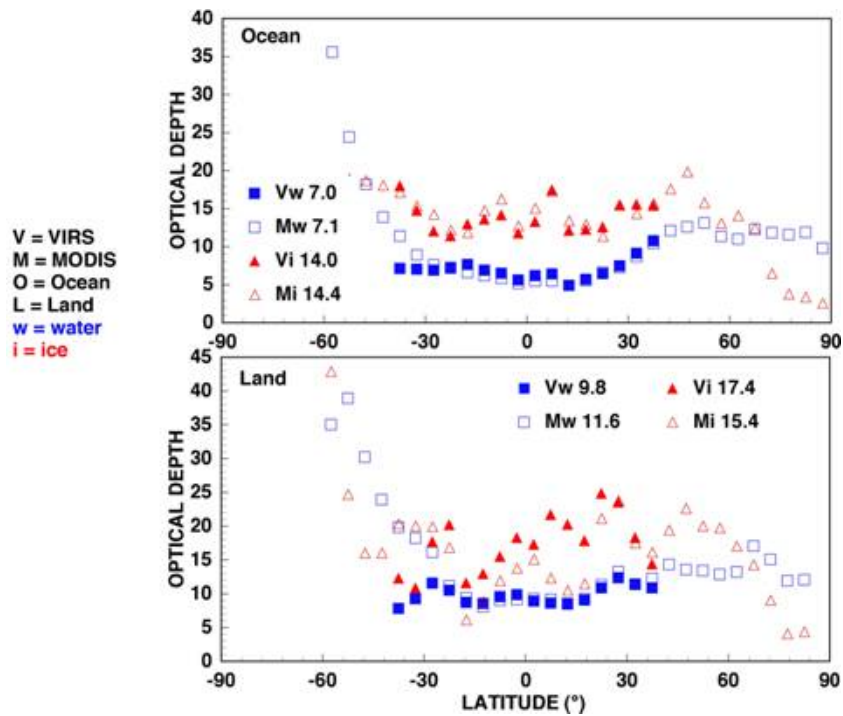


Fig. 14. Zonal mean daytime cloud optical depths from MODIS and VIRS, June 2001.

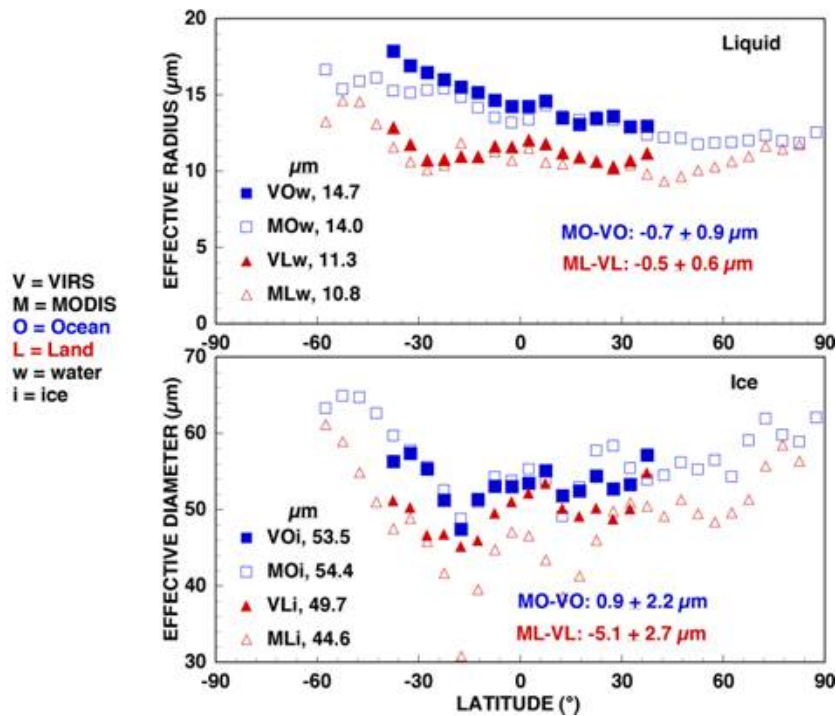


Fig. 15. Zonal mean daytime cloud particle sizes from MODIS and VIRS, June 2001.

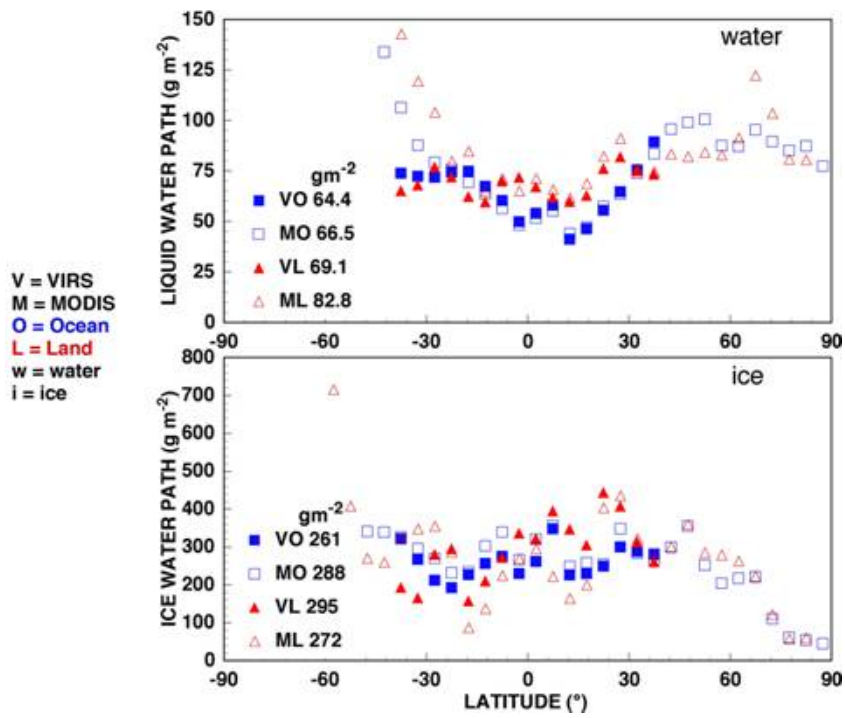


Fig. 16. Zonal mean daytime water paths from MODIS and VIRS, June 2001.

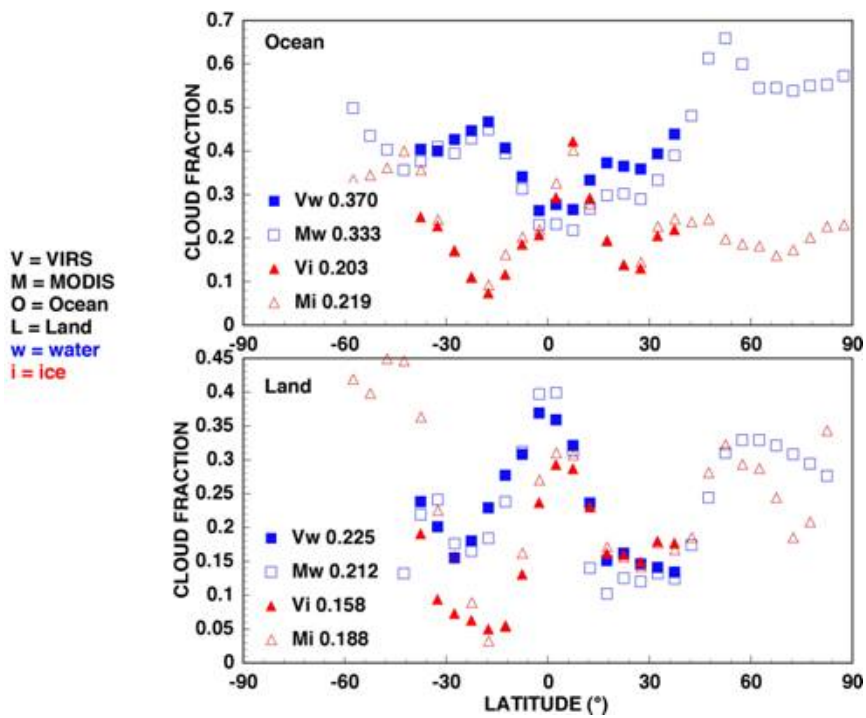


Fig. 17. Zonal mean daytime ice and water cloud amounts from MODIS and VIRS, June 2001.

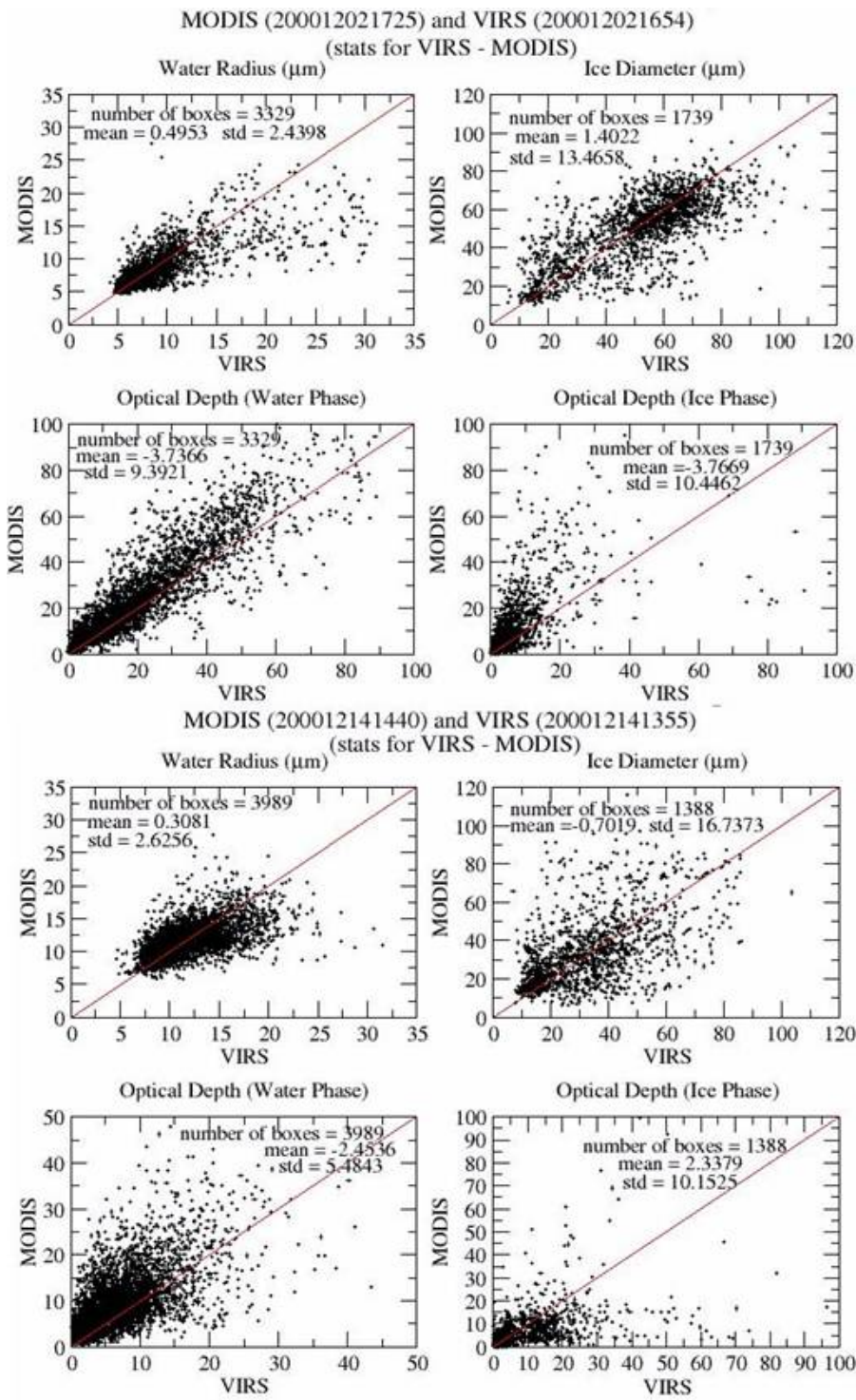


Fig. 18. Averaged 0.25°-region cloud properties from matched MODIS and VIRS, Dec, 2000.



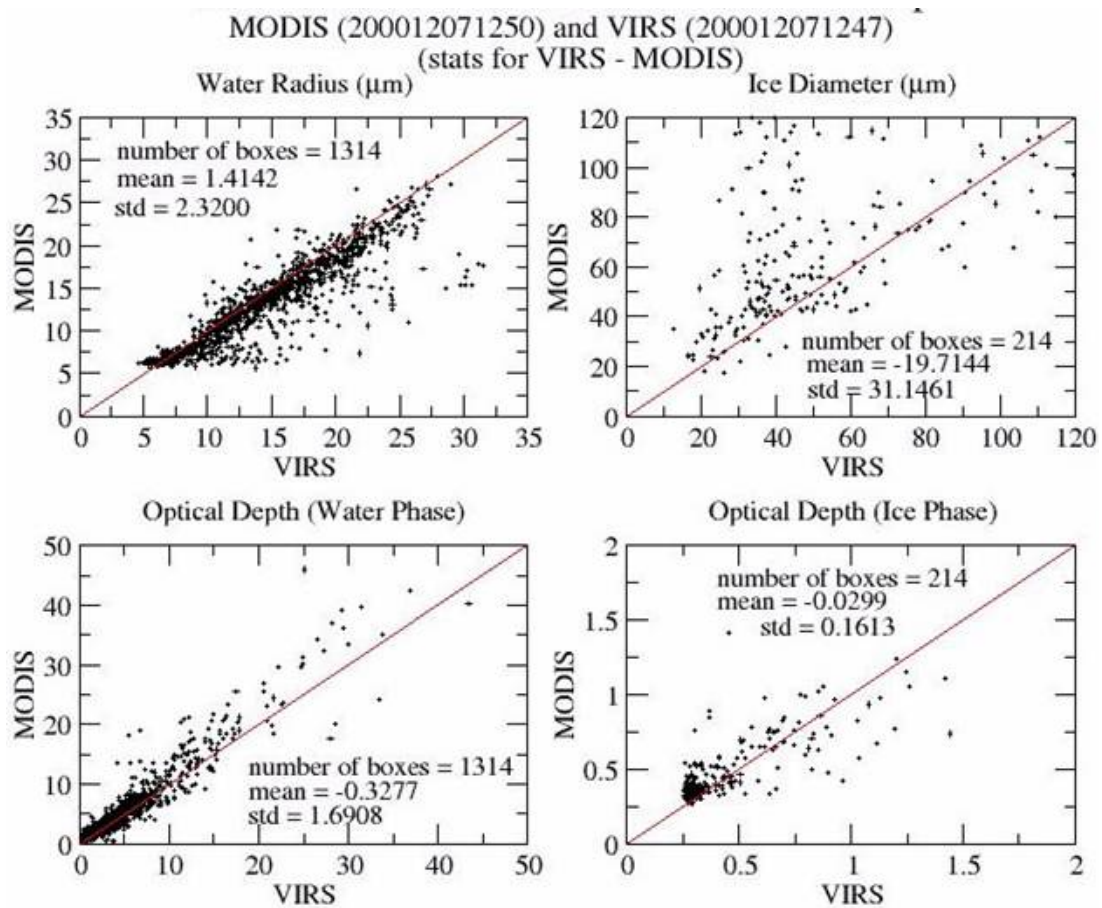


Fig. 19. Averaged 0.25°-region cloud properties from matched MODIS and VIRS, Dec, 2000.

Return to Quality Summary for: [SSF Terra Edition1A](#)